J Comp Physiol A (1991) 168:1–12

Journal of Comparative Physiology A Sensory, Neural, and Behavioral Physiology

Gravikinesis in *Paramecium*: Theory and isolation of a physiological response to the natural gravity vector

Hans Machemer[1*], Sigrun Machemer-Röhnisch[1], Richard Bräucker[1], and Keiichi Takahashi[2]

[1] Arbeitsgruppe Zelluläre Erregungsphysiologie, Fakultät für Biologie, Ruhr-Universität, W-4630 Bochum 1, Federal Republic of Germany
[2] Zoological Institute, Faculty of Science, University of Tokyo, Hongo, Tokyo 113, Japan

Accepted October 30, 1990

Summary. 1. We have investigated a physiological component of the gravitaxis of *Paramecium* using established mechanisms of ciliate mechanosensitivity. The horizontal, up and down swimming rates of cells, and the sedimentation of immobilized specimens were determined. Weak DC voltage gradients were applied to predetermine the *Paramecium* swimming direction.

2. An observed steady swimming rate is the vector sum of active propulsion (P), a possible gravity-dependent change in swimming rate (Δ), and rate of sedimentation (S). We approximated P from horizontal swimming. S was measured after cell immobilization.

3. Theory predicts that the difference between the down and up swimming rates, divided by two, equals the sum of S and Δ. Δ is supposed to be the arithmetic mean of two subcomponents, Δ_a and Δ_p, from gravistimulation of the anterior and posterior cell ends, respectively.

4. A negative value of Δ (0.038 mm/s) was isolated with Δ_a(0.070 mm/s) subtracting from downward swimming, and Δ_p(0.005 mm/s) adding to upward propulsion. The data agree with one out of three possible ways of gravisensory transduction: outward deformation of the mechanically sensitive 'lower' soma membrane. We call the response a negative gravikinesis because both Δ_a and Δ_p antagonize sedimentation.

Key words: Mechanosensation – Gravitaxis – Kinesis – *Paramecium*

Introduction

Negative gravitaxis[1] in *Paramecium* is a spectacular upward orienting behaviour which has intrigued experimenters and theorists since 100 years (Verworn 1889). The specific density of this cell is about 4% above that of common freshwater (Taneda 1987) which would induce slow sedimentation of cell populations in the absence of compensating mechanisms. Oriented upward swimming of *Paramecium* was claimed to be effected by physical mechanisms (such as buoy-principle, hydrodynamics of small bodies, dislocation between centers of effort and gravity), or involving sensory transduction (reviewed by Bean 1984; Haupt 1962; Machemer and De Peyer 1977). A large body of controversial and apparently inconclusive data on gravitaxis in the early literature seems to have discouraged the search for guiding mechanisms for decades. Since cellular electrophysiology has become applicable to ciliates, gravireception can be viewed in the light of mechanosensory transduction located in the soma membrane (Naitoh and Eckert 1969; see Machemer and Deitmer 1985). The bipolar organization of this mechanosensitivity favours a classical view of physiologically mediated gravitaxis, the statocyst hypothesis (Loeb 1897; Lyon 1905). Recent gravitaxis experiments in *Paramecium* and invertebrate larvae in fact suggest the existence of a gravity-induced cellular motor response (Mogami et al. 1988a, b; Baba et al. 1989). The present study takes a combined theoretical and experimental approach to cellular gravitaxis. Proceeding on established grounds of ciliary electromotor coupling, we postulate, that a gravity stimulus modulates the steady-state membrane potential and hence affects ciliary frequency, and the rate of forward swimming in *Paramecium*. We have designed mass experiments and have taken extensive methodical steps to isolate and secure a gravity induced motor response. Our data prove the existence of a negative gravikinesis in *Paramecium* and

Abbreviations: Δ gravity-induced change in active propulsion; Δ_a change in active propulsion as induced by anterior gravireceptor; Δ_p change in active propulsion as induced by posterior gravireceptor; D rate of downward swimming; D_i individual downward swimming rate; n number of data; P active propulsion of cell; Φ mean swimming angle; p probability; R scalar value of mean swimming rate; r_0 coefficient of orientation; r_t coefficient of taxis response; S rate of sedimentation; β_i individual angle of swimming direction; U rate of upward swimming; U_i individual upward swimming rate; v_i individual swimming rate

* To whom offprint requests should be sent

[1] Traditionally, the term of 'geotaxis' was used in the literature. Because gravity is not restricted to terrestrial environments, 'gravitaxis' has now been commonly adopted as a descriptive term

present a testable theoretical outline of transduction of the gravity stimulus. Preliminary data have been published in abstract form (Machemer 1989, 1990a; Machemer-Röhnisch 1989; Bräucker and Machemer-Röhnisch 1990).

Theory

Bipolar mechanosensitivity. The anterior and posterior ends of the cell soma of *Paramecium* are sites of high mechanosensitivity. Activation of anterior Ca mechanoreceptor channels generates a depolarizing receptor potential, similar stimulation of posterior *K* mechanoreceptor channels hyperpolarizes the membrane (Machemer and Ogura 1979). Simultaneous deformation of mechanically sensitive areas of the soma leads to summing of receptor potentials. Favourable cable conditions in *Paramecium* spread the receptor potential involving virtually no losses, so that the motor response is activated simultaneously in the cilia. The polarity and amplitude of the receptor potential determine the type of the ciliary motor response (Machemer 1988a, b). Minor depolarizations decrease the rate of forward swimming, minor hyperpolarizations slightly enhance forward swimming (Machemer and Sugino 1989).

We consider the possibility that the raised density of the cytosol (with respect to that of the medium) and its non-ideal viscous properties tend to deform the apical membrane inward (net force directed inward), and the 'bottom' membrane outward (net force directed outward). Therefore, gravity may affect the anterior or posterior mechanoreceptors or both. We anticipate that activated anterior and/or posterior receptor conductances generate a tonic depolarizing, hyperpolarizing or no receptor potential at all, depending on cell orientation and adequacy of stimulation. In principle, the receptor membrane may be responsive to one out of at least 3 types of gravity-induced mechanical load: (1) from both outside and inside the cell, (2) from outside only, and (3) from inside only.

Elements of gravity-induced swimming. Locomotion of a ciliated cell results from the vector sum of two forces: propulsion by ciliary activity (*P*) and sedimentation (*S*).

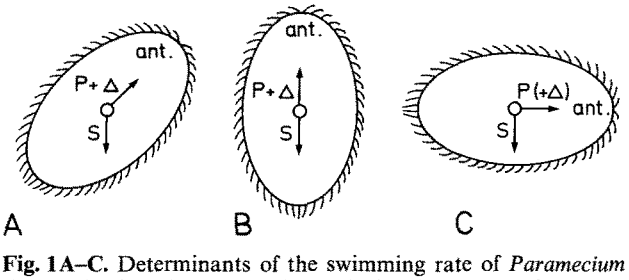

Fig. 1A–C. Determinants of the swimming rate of *Paramecium* in the gravity field (ant. = anterior end of cell). Vectors of active propulsion (*P*) and (downward) sedimentation (*S*) may be supplemented by a gravity-induced kinetic component, *Δ*, which adds to, or subtracts from *P*. **A.** $P+\Delta$ may take any direction depending on cell orientation. **B.** In upward swimming cells, the effective swimming rate is determined by direct subtraction of *S* from $P+\Delta$; during downward swimming, *S* adds to $P+\Delta$. **C.** Sedimentation is not represented in a horizontal swimming trace; *Δ* is minimal or virtually absent (so that *P* is approximated)

If the cell can sense the gravity stimulus and respond to it, a stimulus increment (or decrement) will add to propulsion ($P+\Delta$) (Fig. 1A). If the cell moves vertically, the contributions of S, Δ and *P* add numerically (Fig. 1B). *S* does not affect horizontal displacement, and *Δ* approximates zero during horizontal locomotion; minimal values of *Δ* may nevertheless persist under certain conditions (Fig. 1C; see Discussion).

Three alternative models of sensory-motor coupling under gravity

Assuming that the cytosol acts as a heavy body of non-ideal fluid which tends to deform the top and bottom membrane, an inward pressure component exists across the upper membrane; the pressure is directed outward across the lower membrane.

Model #1 assumes that inward as well as outward deformation of the sensitive membrane is an adequate stimulus for gravitransduction, and that the electric membrane response is related to stimulus size (directed inward or outward) over the sensitive area of the membrane (Fig. 2 left). During downward swimming (*D*) the speed of locomotion is determined by propulsion (*P*), sedimentation (*S*), a gravity-induced hyperpolarizing conductance increase at the posterior cell end which induces an increment in propulsion (Δ_p), and a gravity-induced depolarizing conductance increase at the anterior end, inducing a decrement in propulsion (Δ_a):

$$D\downarrow = P\downarrow + \Delta_p\downarrow + \Delta_a\uparrow + S\downarrow. \quad (1)$$

Similar conditions apply during upward swimming (*U*) (Fig. 2 middle):

$$U\uparrow = P\uparrow + \Delta_p\uparrow + \Delta_a\downarrow + S\downarrow. \quad (2)$$

where Δ_a and sedimentation act opposite to propulsion *P* and Δ_p. Addition of Eqs. (1) and (2) give:

$$D\downarrow + U\uparrow = 2S\downarrow, \quad \text{or} \quad (D-U)/2 = S. \quad (3)$$

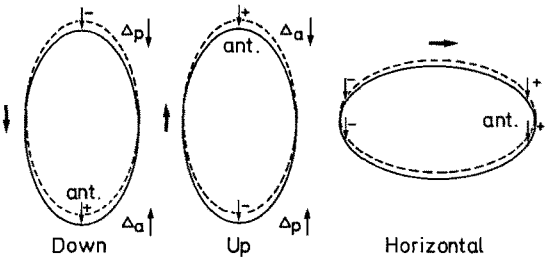

Fig. 2. Gravitransduction according to model #1. Inward and outward deformation (*thin arrows*) of the mechanically sensitive soma membrane can elicit a gravireceptor response (+: depolarizing; −: hyperpolarizing). *Left:* During downward swimming (*heavy arrow*), hyperpolarizing activation of posterior gravireceptors tends to raise the swimming rate ($\Delta_p\downarrow$), and depolarizing activation of anterior gravireceptors tends to decrease the swimming rate ($\Delta_a\uparrow$). The summed values of $\Delta_p\downarrow$ and $\Delta_a\uparrow$ add to propulsion and sedimentation (Eq. 1). *Middle:* Similar relationships apply to upward swimming (Eq. 2). *Right:* During horizontal swimming, the gravitational load on the anterior and posterior ends of the cell is minimal so that the net gravikinetic response approximates zero, and the active propulsion (*P*) is represented by the net swimming rate

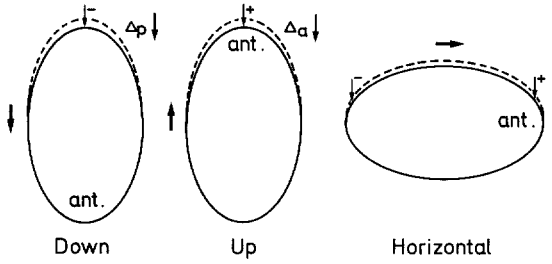

Fig. 3. Gravitransduction according to model #2. Only inward deformation of the sensitive anterior and posterior membrane can cause gravitransduction. In this model $\Delta_p\downarrow$ and $\Delta_a\downarrow$ share the positive sign with sedimentation enhancing the downward swimming rates. Other definitions corresponding to Fig. 2. See Eqs. (5) and (6)

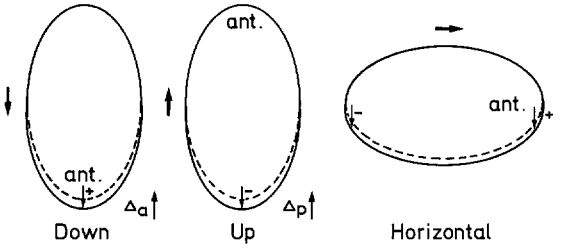

Fig. 4. Gravitransduction according to model #3. Only outward deformation of the sensitive anterior and posterior membrane can cause gravitransduction. In this model $\Delta_p\uparrow$ and $\Delta_a\uparrow$ share the same sign, but unlike model #2, they antagonize sedimentation during swimming. Other definitions corresponding to Fig. 2. See Eqs. (8) and (9)

Model #1 predicts that the rate of sedimentation will be 50% of the difference between down and up swimming rates. Equation (3) is valid also for the cases where the absolute amounts of Δ_p and Δ_a are different, or one subcomponent or both Δ_p and Δ_a are nil.

During horizontal swimming the mechanical load on the sensitive anterior and posterior membranes will be at minimum (Fig. 2 right). In *Paramecium*, stimuli applied to these areas polarize the membrane inversely so that we assume, as a first approximation, that Δ_p and Δ_a cancel out, and horizontal swimming approximates active propulsion (P). Then, subtraction of Eq. (2) from Eq. (1) leads to:

$$(D+U)/2=P. \tag{4}$$

Equation (4) states that horizontal swimming corresponds to the arithmetic mean of downward and upward swimming. Applicability of model #1 to gravisensation in *Paramecium* can be tested by determinations of D, U, P and S, and using the Eqs. (3) and (4).

Model #2 differs from model #1 in that it assumes gravisensory transduction only by *inward* deformation of the membrane (Fig. 3). Δ_p and Δ_a share the positive sign with sedimentation enhancing the downward swimming rates. Downward and upward swimming (Fig. 3, left, middle) are now defined as follows:

$$D\downarrow=P\downarrow+\Delta_p\downarrow+S\downarrow, \quad \text{or } \Delta_p=D-P-S; \tag{5}$$

$$U\uparrow=P\uparrow+\Delta_a\downarrow+S\downarrow, \quad \text{or } \Delta_a=P-U-S. \tag{6}$$

Addition of Eqs. (5) and (6),

$$(D-U)/2=S+(\Delta_p+\Delta_a)/2, \tag{7}$$

shows that with model #2 the difference between D and U, divided by 2, exceeds sedimentation by the arithmetic mean of Δ_p and Δ_a which is equal to the value of Δ (Fig. 1). Applicability of model #2 can be tested by measurements of D, U, P and S. Stimulus conditions during horizontal swimming correspond to those of model #1 so that the value of P is approximated. If the data show that $(D-U)/2>S$, the scalar values of Δ_p and Δ_a are derived from Eqs. (5) and (6).

Model #3 assumes that gravisensory transduction acts by outward deformation of the sensory membrane (Fig. 4). Like in model #2, Δ_p and Δ_a have the same sign, but different from that model, they antagonize sedimentation during swimming. Downward and upward swimming are now defined as:

$$D\downarrow=P\downarrow+\Delta_a\uparrow+S\downarrow, \quad \text{or } \Delta_a=P-D+S; \tag{8}$$

$$U\uparrow=P\uparrow+\Delta_p\uparrow+S\downarrow, \quad \text{or } \Delta_p=U-P+S. \tag{9}$$

Addition of Eqs. (8) and (9) give

$$(D-U)/2=S-(\Delta_p+\Delta_a)/2. \tag{10}$$

Equation (10) predicts that $(D-U)/2<S$.Hence, model #3 differs from models #1 and #2, and can also be tested experimentally. Stimulus conditions during horizontal swimming are comparable to models #1 and #2 allowing to approximate P. Additional determinations of D, U and S give the scalar values of Δ_p and Δ_a.

Selection of the appropriate model. Statistically significant values of the half-difference between downward and upward swimming rates, and sedimentation, are the crucial experimental parameters determining which model is valid. If $(D-U)/2$ equals S, model #1 is appropriate, or the swimming rate was unaffected by gravity. Model #1 does not resolve the fractional contributions of the anterior and posterior gravireceptors to motility. If $(D-U)/2$ is shown to be unequal to S, either model #2 ($>S$) or model #3 ($<S$) can apply. The sign and size of the arithmetic mean of Δ_p and Δ_a are generalized gravikinetic values, which may be expressed by Δ (Fig. 1):

$$\Delta=(\Delta_p+\Delta_a)/2. \tag{11}$$

Basic equation of vertical swimming. Paramecium cells can be induced to swim downward or upward by application of a vertical DC voltage gradient. The cells head toward the cathode irrespective of their location at the bottom or top of the fluid space (Fig. 5). Specificity of the mechanoreceptor prevents interference of weak voltage stimuli. A low level of the applied voltage gradient also keeps potential-sensitive ciliary responses below saturation (Machemer 1988c).

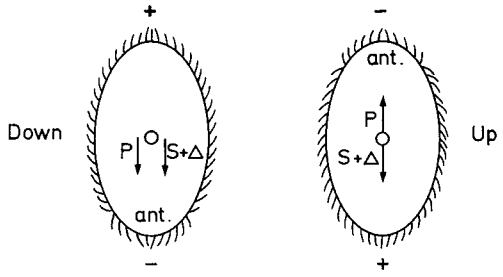

Fig. 5. Induction of downward and upward swimming applying a vertical DC voltage gradient (0.6 V/cm). During galvanotaxis, a cell swims forward heading toward the cathode. Simple switching of polarity of the voltage gradient reorients swimming from 'Down' to 'Up'. *P*, *S* and *Δ* add or subtract comparable to Fig. 1B

Figure 5 shows that the downward swimming rate is the vector sum of *P*, *S* and *Δ* (Eq. 12). The same applies to upward swimming with the direction of *P* reversed and the sign of *Δ* not reversed (Eq. 13; see models #2 and #3). Summing of Eqs. (12) and (13) leads to Eq. (14), which expresses that the difference between downward (*D*) and upward swimming (*U*), divided by 2, gives the sum of sedimentation and the gravity-induced mean kinesis, *Δ*:

$$D\downarrow = P\downarrow + S\downarrow + \Delta \tag{12}$$

$$U\uparrow = P\uparrow + S\downarrow + \Delta \tag{13}$$

$$D\downarrow + U\uparrow = 2(S\downarrow + \Delta),$$

$$\text{or } (D-U)/2 = S + \Delta. \tag{14}$$

Equation (14) represents Eqs. (3), (7) and (10) in a generalized form. The resulting sign and value of *Δ* identify the type of gravisensory transduction (models #1 to #3) and determine the direction and size of gravikinesis.

Materials and methods

Culture. Wild-type of *Paramecium caudatum* were reared in Cerophyl solution (Cerophyl Laboratories, Inc., Kansas City; 0.2% w/v cerophyl powder in aqua bidest., autoclaved), buffered at 7.0 pH by Sörensen buffer (1.8 m*M* Na_2HPO_4 + 0.2 m*M* KH_2PO_4), bacterized with *Aerobacter aerogenes*, cultured at 22° C in 14 h/10 h light regimen, and harvested in early stationary phase after 2 days.

Transfer to experimental solution. Cells were washed and collected after negative gravitactic accumulation in a column of experimental solution (1 m*M* $CaCl_2$ + 1 m*M* KOH + 1.6 m*M* MOPS acid, pH 7.0). This washing procedure was repeated once, then the cells were infused into the experimental chamber (Fig. 6). Smooth transfer to the chamber of minimally agitated cells was achieved by 3 cm level difference of the solutions.

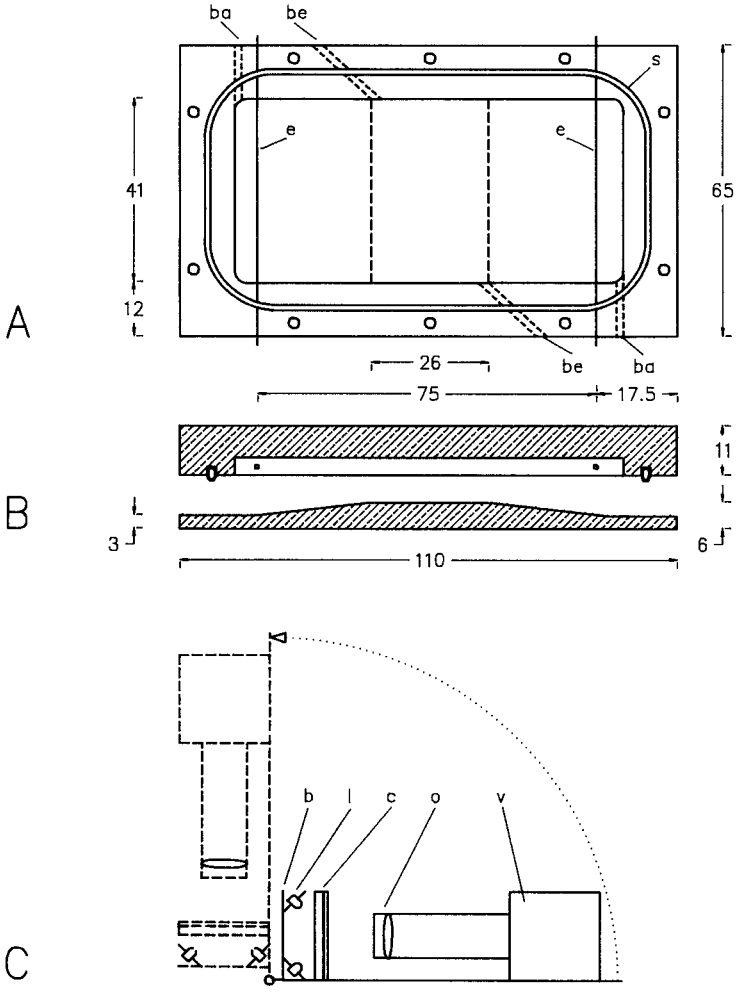

Fig. 6A–C. Setup for recording graviresponses. **A.** Chamber (plexiglass; surface view) with dimensions in mm as indicated. The well includes a central part, 26 mm wide, for the experimental solution (entry: *be*) and two peripheral sections, which include the electrodes (*e*; 75 mm apart) and are filled with 1.5% agar in experimental solution through a bore (*ba*). A silicone rubber seal (*s*) surrounding the well is tightened by 8 screws connecting cover and bottom of the chamber. **B.** Longitudinal section across chamber bottom and cover showing reduction to 1.6 mm height in the central part of the well. A 25-μm O_2 and CO_2-permeable transparent foil intervenes between chamber bottom and cover (not shown). Omitted are also bores (3 mm in diameter) perforating the cover for access of air to the intercalated foil. **C.** Principle of recording vertical (continuous lines) and horizontal cell movement (dashed lines). A macro-objective (*o*) of the videocamera (*v*) focuses on the central area of the chamber (*c*), which receives oblique illumination (*l*) against a black background (*b*)

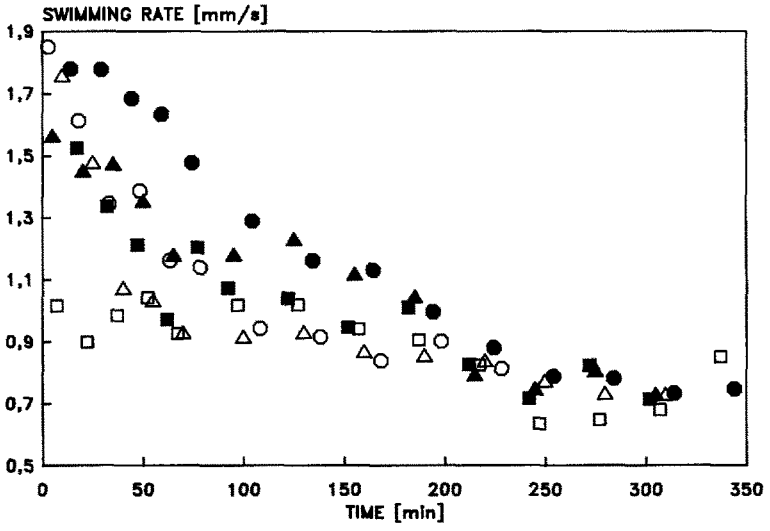

Fig. 7. Variables affecting rates of horizontal swimming in the experimental chamber. The effects of culturing time (2 days: *open symbols*; 6 days: *closed symbols*), and time of ionic equilibration prior to incubation (up to 14 min: *circles*; 3 h: *triangles*; 16 h: *squares*) were tested to determine the appropriate time of cell incubation in the chamber before starting the experimental sequence. Swimming rates decreased during a period of 4 h and settled near 0.8 mm/s. The slow relaxation of swimming was largely independent of the time of incubation in the experimental solution suggesting that it was primarily determined by the O_2-CO_2 balance in the chamber. Motion affected by the closed chamber environment, was at steady-state after 4 h of incubation

Equilibration. A sample of about 200 cells was equilibrated and left unstirred for 4 h in the chamber. During equilibration the chamber was kept in a water-saturated atmosphere at 22° C. An equilibration time of 4 h is advised to secure full electrochemical equilibrium of the cell after transfer to a modified ionic environment (Oka et al. 1986; see Machemer 1990b). The same time was required for establishing a steady-state in O_2-CO_2 balance and hence swimming rate in the chamber environment (Fig. 7). Care was taken to fully isolate vibration from the chamber until the end of the experiment.

Immobilization of cells. For determination of the sedimentation rate, samples of cells were exposed to a solution of 1 m*M* $NiCl_2$ in experimental solution after the end of the active swimming period (Fig. 8).

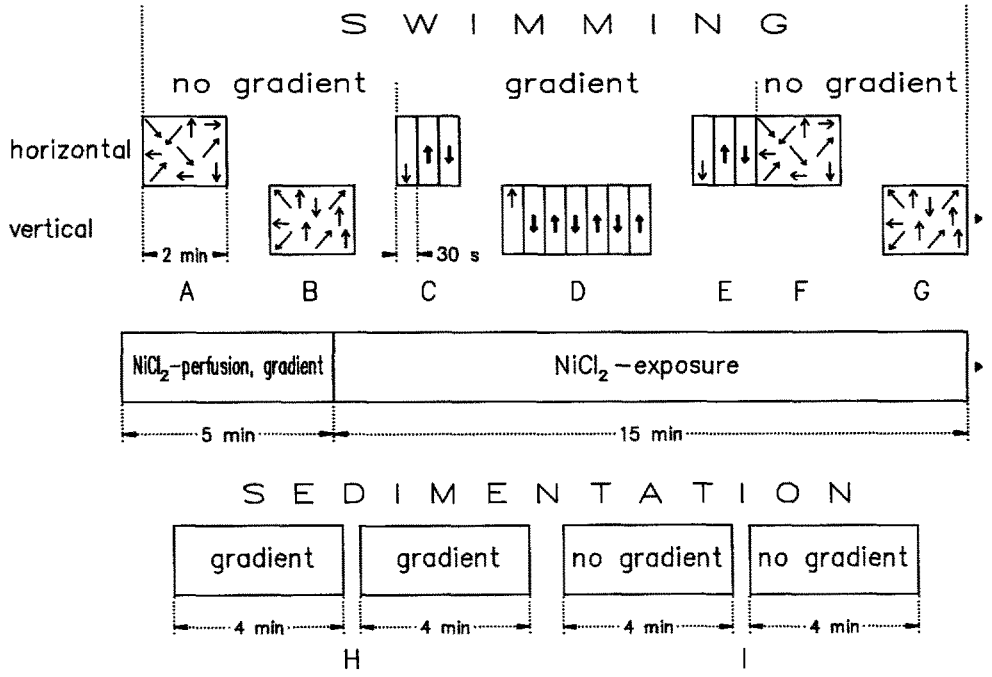

Fig. 8. Experimental protocol for determination of the rates of swimming and sedimentation. The procedure is represented by time bars (read in rows from left to right). Recording starts with the chamber oriented horizontally (A) and then vertically (B, both unbiased swimming). The voltage gradient is turned on after 5 min to collect cells near the cathode (light arrow), followed by two 30 s sequences of swimming in opposite directions (C; heavy arrows). The chamber is then gradually reoriented by 90°, and the gradient is turned on to collect cells up; 3 pairs of 30 s down and 30 s up swimming are recorded (D). The chamber is reoriented horizontally, the gradient turned on to collect cells down, and a pair of horizontal swimming recorded (E). Further experiments recording unbiased horizontal (F) and vertical swimming (G). The chamber is perfused for 5 min with 1 m*M* Ni^{2+} in experimental solution while the voltage gradient is on to save active cells from being swept out of the chamber. The cells are immobilized after further 15 min of exposure to Ni^{2+}. Sedimentation of the immobilized cells with the voltage gradient on is recorded during two time intervals of 4 min each (H). A second pair of 4-min sedimentations of the same preparation occurs with the gradient turned off (I). Seven parameters and circumstantial conditions were tested: 1. spatial symmetry of the chamber (A); 2. effects of time (A, F; B, G; C, E); 3. effect of the voltage gradient on swimming rate (A, C; E, F); 4. horizontal versus vertical swimming (C, D, E); 5. down versus up swimming (D); 6. completeness of cell immobilization (H, I); 7. rate of sedimentation (H, I)

An amount of 8 ml of Ni^{2+}-solution (corresponding to 5 chamber volumes) was slowly infused by gravity force from the lower side of the vertically oriented chamber. In order to reduce the loss of cells, a voltage gradient of 0.6 V/cm (cathode down) was applied for 5 min to accumulate active cells against the direction of infusion. At the end of the infusion period, 15 more min were allowed for completion of cell immobilization. According to microscopic tests, a minor fraction of cells (<1%) shows residual ciliary activity after this time. Immobilized cells settle preferentially with their long axes vertical and their rear ends down (Kuznicki 1968; Roberts 1970), and this applies to young cultures in the first line. In Ni^{2+}-immobilized cells from 2-day cultures, Taneda et al. (1987) counted 66% of the specimens in vertical (±20°) sectors and 14% in horizontal (±30°) sectors. Roberts (1970) inferred a maximal velocity variation of 30% related to orientation for *Paramecium*. Because the majority of immobilized cells settles at vertical orientation, the remaining fraction of specimens at oblique and horizontal orientations does not significantly shift the median of the sedimentation rate (see Fig. 13). This conclusion receives additional support from the low Reynolds number ($<10^{-1}$) of protozoan cells.

Voltage gradient and galvanotaxis. A DC voltage gradient (0.6 V/cm) was applied during part of the swimming and sedimentation experiments. The gradient was stabilized using a constant current source supplying ±150 VDC for regulation. The current was calibrated so as to generate the predetermined voltage drop across the medium. Persistence of the current was monitored during the experiment. Generation of a voltage gradient by means of constant current overcomes time-dependent instabilities of the electrodes. The gradient of 0.6 V/cm (or 14 mV per cell length) corresponds to a maximal cathodal depolarization of 7 mV (and maximal anodal hyperpolarization of the same size) for a cell oriented parallel to the field lines. Thus, the applied gradient is a weak electric stimulus (Machemer 1988b).

Chamber. The experimental vessel (65 × 110 × 15 mm outer dimension; Fig. 6) includes a fluid space of 41 × 85 × 1.6 mm or 5.6 cm^3. This volume was aerated by diffusion using a gas-permeable 25 µm foil (Biofoil 25, Heraeus, Hanau) intercalated between the well and the perforated plexiglass cover (138 bores of 3 mm diameter). The aerated area of the fluid space corresponds to a 1.8 cm^{-1} surface-to-volume ratio equivalent to the upper surface of a 5.5 mm deep well in a circular Petri dish. Aeration strongly affects the swimming rate of the cells (Fig. 7). A 1.6 mm depth of the fluid space was chosen to minimize hydrodynamic wall effects (unstirred layer) on swimming rates and to secure focus for video recording of the cells. Chlorided silver wires were inserted at a distance of 75 mm from each other, in order to generate a linear voltage drop across the longer axis of the chamber. The electrodes were embedded in 1.5% agar in experimental solution. A central 8.5 × 11.5 mm field of the chamber was used for recording of swimming cells (for sedimentation: 4 × 5 mm field). Prior to transfer of the cells, the chamber was filled with experimental solution to avoid the inclusion of air bubbles. The cells were laterally illuminated by infrared-filtered light.

Recording. Cell movements were recorded using a CCD-videocamera (Panasonic F10) with 25 Hz framing rate connected to a macro-lens. Essential parameters such as date, time (10 ms resolution), horizontal or vertical orientation of chamber, and gradient polarity were superimposed on the video field for identification of the experiments.

Experimental schedule. Figure 8 explains the sequence of experimental steps to record the swimming rates and sedimentation of a sample of about 100 cells. The schedule includes tests for: (1) existence of a spatial asymmetry of the chamber (in terms of physical and/or chemical properties), which might affect the up and down swimming rate; (2) the effect of time on swimming rate; (3) the effect of the voltage gradient on swimming rate; (4) horizontal and vertical swimming rates; (5) down and up swimming rates; (6) completeness of cell immobilization, and (7) rate of sedimentation. After turning on the voltage gradient of 0.6 V/cm, a 30 s period was allowed for cathodal accumulation of cells. The same gradient was applied (cathode up) during the sedimentation period to provide improved separation of remaining active cells from fully immobilized cells. Care was taken to avoid mechanical disturbances of the cells during changes between horizontal and vertical orientation of the chamber; a time of up to one minute was allowed for this 90°-reorientation.

Digital image analysis. Our processing of video records involves two automatic and one semi-automatic steps:

1. Digitization of every 5th video-field (200 ms intervals; 512 × 256 pixels; 256 intensity levels; RDDK-card, Bartscher, Eschwege); storage on hard disk together with time information.
2. Application to digitized fields of background-recognition algorithm, filtering (area-sensitive and common skeleton procedure) for isolation of cell shapes; superposition of 20 frames using colour sequence to show time.
3. Marking of track start and end points by operator; automatic identification of cell boundaries, and monitoring of time sequence and steadiness of swimming speed by program; automatic calculation of time intervals, length and angle of tracks, and swimming rates; automatic data storage.

Statistics. For evaluation, we employ methods of non-parametric statistics because the distributions of swimming rates and angles of locomotion are unknown. Data samples are represented by median; 95% confidence intervals describe distribution ranges. Experimental units (Fig. 8 A, F), (B, G), (C, E) were compared using the Mann-Whitney *U*-test (two-tailed error probability of 5%; Sachs 1984) to test for potential differences of the medians. Similar checks were done for the existence of a spatial bias of the experimental chamber (horizontal swimming rates in units C, F), and completeness of immobilization (units H, I).

Model #1 postulates the identity of the up and down swimming rates after compensation for sedimentation. Model #1 is tested according to Eq. (3) by comparison of the medians of individual $(D_i - S)$ and $(U_i + S)$ values. A statistically secured difference between these means rejects model #1 and confirms the existence of Δ.

Means of angles, and coefficients of orientation and taxis. The mean of directional data (individual angles β_i; n = number of data) is described by the mean angle Φ and the value of the mean vector R (Batschelet 1981). The coordinates of the 'centre of mass' (x, y) are calculated as:

$$x = \frac{\sum(\cos\beta_i)}{n}; \quad y = \frac{\sum(\sin\beta_i)}{n};$$

$$R = \sqrt{x^2 + y^2};$$

$$\Phi = \begin{cases} \text{if } x > 0\text{: } \arctan(y/x) \\ \text{if } x < 0\text{: } 180° + \arctan(y/x) \\ \text{if } x = 0\text{: special further conditions.} \end{cases}$$

The orienting coefficient r_0 was defined as:

$$r_0 = R\cos\Phi.$$

Hence, $r_0 = +1$, if all cells are strictly oriented up (0°), $r_0 = -1$, if all cells are oriented down (180°), and $r_0 = 0$, if all cells are oriented 90° or 270°.

For evaluation of the angular distribution of swimming rates, the frequency of swimming angles (β_i) together with swimming rates (v_i) must be taken into account. Thus, the values of R and Φ were weighted by the swimming rate:

$$x = \frac{\sum[(\cos\beta_i)v_i]}{n}; \quad y = \frac{\sum[(\sin\beta_i)v_i]}{n};$$

(Definitions of R and Φ as shown above).

A taxis coefficient r_t was defined as:

$$r_t = \frac{-R \cdot n \cdot \cos \Phi}{\sum v_i}.$$

This coefficient combines the orientational response (=mean angle of orientation) with the kinetic response of the cells. Hence, the coefficient represents the cellular taxis response. The value of r_t equals -1, if *all* cells show *negative* (upward) gravitaxis; it is equal to $+1$, if all cells show *positive* (downward) gravitaxis, and the coefficient equals 0, if a gravitaxis response cannot be confirmed.

Results

Chamber symmetry test

Physical and chemical properties of the fluid volume of the experimental chamber should not convey a bias to cellular swimming rates in the gravity field. The angular distribution of swimming directions and rates of the *horizontally* oriented chamber (see unit A in Fig. 8) were plotted in polar diagrams using 10° unit sectors (Fig. 9). Figure 9A shows that swimming between angles of 270° and 90° ('distal' direction corresponding to 'up' in a *vertically* oriented chamber) was equally frequent, and included similar angular distributions, as swimming between 90° and 270° ('proximal', corresponding to 'down' in the vertical chamber). The mean angle ($n=899$) was 0°. The swimming velocities show an even distribution of directions (Fig. 9B). We express combined angular distributions of frequency and swimming rates by a taxis coefficient (+0.09, horizontal chamber). This coefficient represents the negative y-value of the resulting mean velocity vector (Table 1). A coefficient value of +0.09 suggests that a taxis did not exist in horizontal swimming behaviour.

Table 1. Coefficients related to gravitaxis. We calculate coefficients using the y-values (reversed sign) of frequency-weighted vectors from the data (Fig. 10, see Methods) or ratios of Δ over P (Table 2). The coefficient of gravitaxis incorporates both orientation and kinetic components. Negative sign indicates effect antagonizing sedimentation. Contributions of orientation and kinesis are approximated in fractions of the taxis coefficient. Coefficients of orientation and kinesis do not fully add to −0.23 because values include rounding errors

Experiment	Coefficients of		
	Orientation	Kinesis	Taxis
Vertical, no V-grad.	−0.21(9/10)		−0.23(1/1)
Vertical, V-gradient		−0.03[a](1/10)	
Up, V-gradient		−0.005[b](2/100)	
Down, V-gradient		−0.06[c](3/10)	

[a] value of Δ divided by horizontal swimming rate (P)
[c] value of Δ_p divided by P
[d] value of Δ_a divided by P

Time effects

Several time-dependent variables may affect cellular locomotion: age of the *Paramecium* culture, length of the ionic equilibration period in experimental solution, and incubation time in the fluid volume of the chamber (Fig. 7). The culturing period (2 and 6 days since start of the culture) had no perceptible effect on the swimming rate (compare open symbols with closed ones), which stabilized near 0.8 mm/s after 4 h of incubation in the chamber. Ionic equilibration (prior to incubation) was not sufficient to achieve steady swimming rates; in any case it took 4 h of incubation in the chamber to stabilize swimming rates. The test (Fig. 7) suggests that a stable

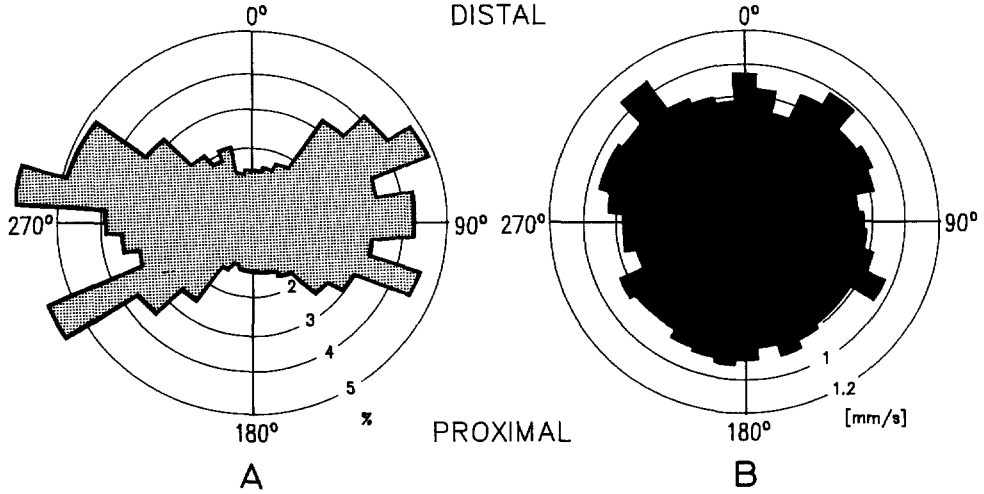

Fig. 9A, B. Unbiased horizontal swimming ($n=899$) as represented in polar distribution diagrams of frequency of swimming directions (**A**) and rates (**B**). The field was divided into 10° sectors. An angle of 0° corresponds to the orientation of 'distal' (equivalent to 'up' in the vertical swimming mode), and 180° correspond to 'proximal' (corresponding to 'down' in the vertical mode). **A.** Frequencies of orientations are the same in the proximal and distal halves of the diagram (resulting vector: 0.07 at an angle of 0°; no laterality!). Preponderance of laterally swimming cells reflects dimensions of the chamber fluid volume (Fig. 6) and screen dimensions for evaluations. **B.** Median swimming rates of sectors distribute evenly (resulting vector: 0.1 mm/s, frequency-weighted angle of 230°). The taxis coefficient of +0.09 suggests absence of directionality

physico-chemical environment, in particular a saturating O_2-CO_2 gas exchange across the chamber membrane, exists after 4 h of incubation of cells in the chamber volume (Fig. 6).

The experimental protocol provides tests for unbiased swimming movement before and after recording of vertical swimming under the voltage gradient control (Fig. 8). No differences in the means of horizontal (A, F) and vertical swimming (B, G) were statistically secured, nor were the rates of horizontal swimming including a voltage gradient (C, E) affected by the intervening experiment (D).

Effects of the voltage gradient on swimming rate

The median rate of unbiased horizontal swimming was 0.834 mm/s ($n=899$). Applying the voltage gradient of 0.6 V/cm raised the swimming rate by 36% (1.136 mm/s, $n=1588$; Table 2). Note that the velocity bias of the voltage gradient cancels for determinations of the gravity-induced component Δ (Eq. 14).

Vertical versus horizontal swimming

In the absence of a voltage gradient, cells swam predominantly upward confirming the existence of a negative gravitactic response (Fig. 10A). Angular velocity distributions ranged evenly between 0.8 and 0.9 mm/s (Fig. 10B; $n=1038$) with a median of 0.817 mm/s (Table 2). This median value resembles that of horizontal swimming (0.834 mm/s) excluding the possibility that gravity unilaterally raises or depresses the swimming rate. Frequency-related weighting of the resulting velocity vector in Fig. 10B (0.23 mm/s, 0°) might suggest that velocity tends to be reduced in downward swimming cells, and to rise during upward swimming in accordance with the negative gravitaxis coefficient (-0.23; gravitaxis coefficient in the horizontal state: $+0.09$). The reverse is true: cells heading upward between 270° and 90° were slower than cells swimming downward between 90° and 270° (0.808 mm/s versus 1.045 mm/s), and this divergence grew, when the range of sectors was reduced to 10° (0.815 mm/s versus 1.045 mm/s; Table 2). The preliminary analysis of horizontal and vertical swimming under-

Table 2. *Paramecium* gravikinesis experimental results

Movement	*V*-gradient applied?	*n*	Displacement Rate [mm/s] median (confidence range[a])
Horizontal	no	899	0.834(0.813; 0.835)
Vertical	no	1038	0.817(0.799; 0.835)
Up (270°−90°)	no	674 of 1038	0.808(0.784; 0.829)
Down (90°−270°)	no	364 of 1038	0.843(0.810; 0.881)
Up (355°−5°)	no	49 of 1038	0.815(0.725; 0.937)
Down (175°−185°)	no	19 of 1038	1.045(0.635; 1.246)
Up	yes	1552	1.057(1.034; 1.079)
Down	yes	1512	1.150(1.132; 1.180)
Horizontal	yes	1588	1.136(1.120; 1.154)
Sedimentation	no/yes	1362	0.084(0.081; 0.086)
Δ			0.038
Δ_a			0.070
Δ_p			0.005

[a] 95% confidence interval of the median value

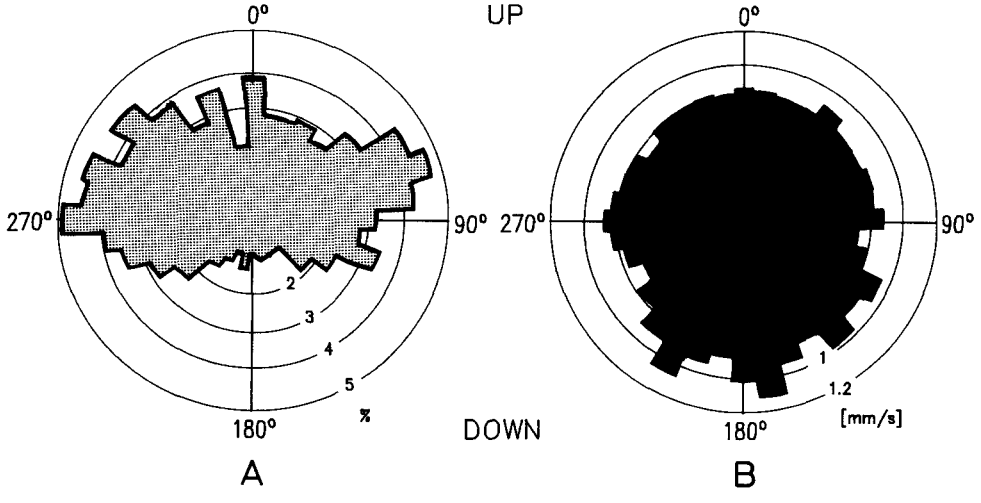

Fig. 10A, B. Vertical swimming in the absence of a voltage gradient ($n=1038$). **A.** Angular distribution of frequency shows a preference of upward swimming. The resulting vector (0.21, 0°) corresponds to upward orientation of swimming. **B.** The angular swimming rates are evenly distributed between 0.8 and 0.9 mm/s (a few cells headed downward near 1 mm/s). The resulting vector (0.23 mm/s, frequency-weighted angle: 0°) shows a moderate upward bias of swimming velocities (taxis coefficient: -0.23) precisely inverse to the gravity vector

scores the need for improved separation of the orientational and kinetic components during gravitactic swimming of *Paramecium*.

Down and up swimming rates

In the presence of a voltage gradient, values of vertical and horizontal swimming rates (horizontal: 1.136 mm/s; up: 1.057 mm/s; down: 1.150 mm/s; Table 2) confirm the shift in velocity obtained without voltage gradient: downward swimming rates were slightly larger, upward swimming rates were smaller than those during horizontal swimming. Polarograms of frequency and velocity illustrate that the voltage gradient acted to restrict swimming directions (Fig. 11A, C) and rates (Fig. 11B, D) to approximately $\pm 15°$ from the vertical axis. Swimming rates outside the $\pm 15°$ sector were rare).

With $n \geq 1500$, the Up and Down swimming rates were clearly separated from each other ($P < 0.001\%$; Fig. 12A; Table 2); the overall range of velocities corresponds to that seen in horizontal swimming (Fig. 12B). Because sedimentation subtracts from upward swimming, and adds to downward swimming, the observed difference in net up and down rates might be effected by the gravity vector. We have tested this possibility adding the sedimentation rate (0.084 mm/s; Table 2) to the Up-value, and subtracting the same rate from the Down-value. The resulting values of active propulsion (Up: 1.141 mm/s; Down: 1.066 mm/s) are still statistically significant ($P < 0.001\%$), and are thus a strong indication for a physiologically mediated cellular response to gravity.

Completeness of immobilization, and absence of electrophoresis

Cells, which are exposed to 1 m*M* $NiCl_2$ for 20 min, become immobilized with their morphological properties unchanged. Preliminary tests have shown that some cells retain a fraction of active cilia, which might convey an undesirable bias to the sedimentation data. We have applied a voltage gradient of 0.6 V/cm to the immobilized cells (cathode up) expecting that the remaining minor population of active cells tends to swim against sedimentation thereby distorting the sedimentation distribution histogram (Fig. 13). Sedimentation rates of the same cells

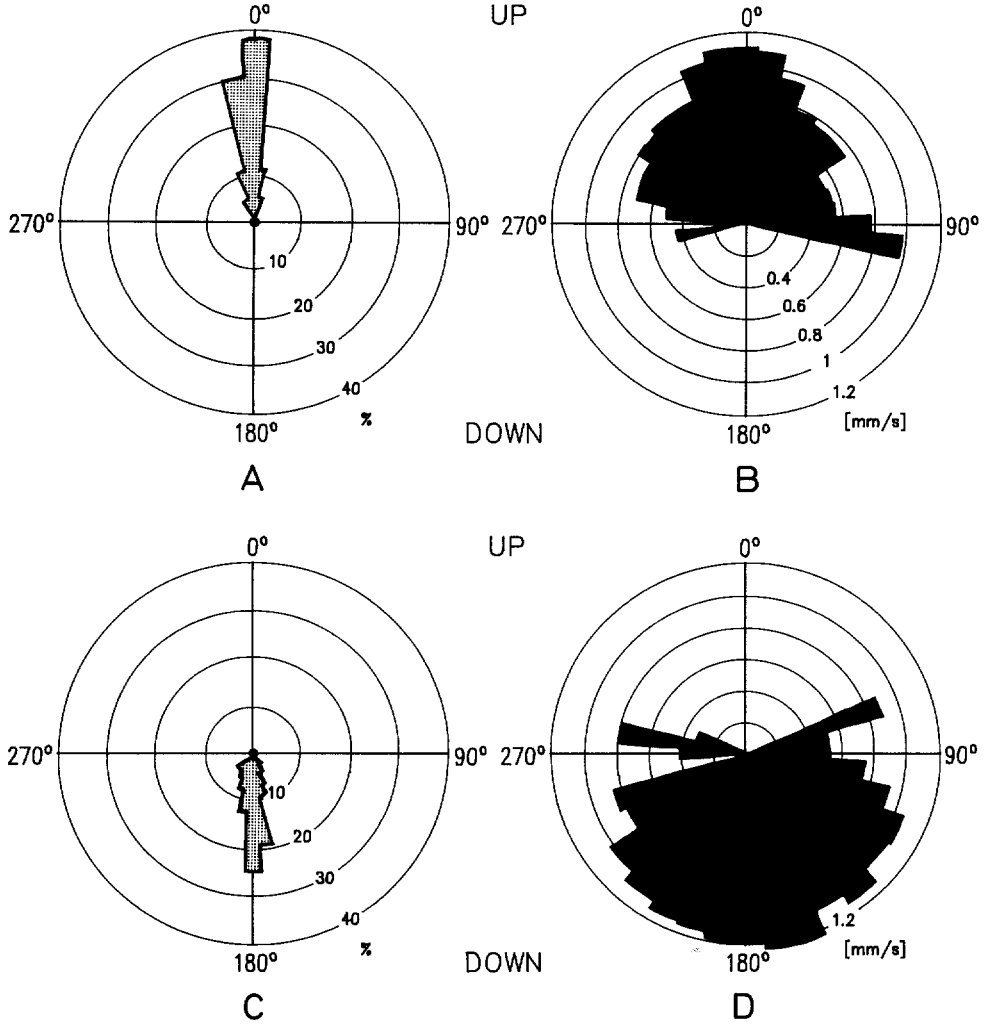

Fig. 11A–D. Vertical swimming (**A, B**: upward, $n = 1552$; **C, D**: downward, $n = 1512$) in the presence of a voltage gradient (0.6 V/cm; cathode and swimming direction coincide). **A.** Upward swimming was largely limited to $\pm 15°$ of the 0°-line (resulting vector: 0.95, 0°). **B.** Angular distribution of swimming rates with the cathode up. The resulting vector was 1.02 mm/s at a frequency-weighted angle of 0°. Note that lateral and even downward swimming did occur in a very small number of cells. The taxis coefficient of -0.95 indicates a near perfect upward orientation, which is based, in this case, on galvanotaxis. **C.** Frequency pattern of downward swimming angles is inverse to that of upward swimming (resulting vector: 0.87, 170°). **D.** Distribution of swimming rates with the cathode down is inverse to (**B**). Resulting vector: 0.85 mm/s, 180°; taxis coefficient: +0.85

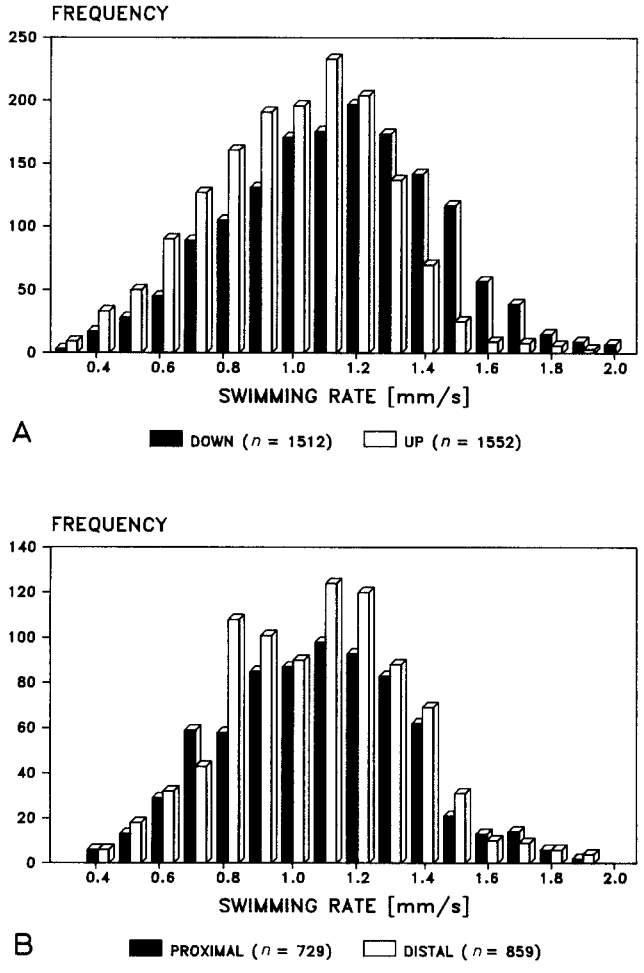

Fig. 12A, B. Histogram representing swimming rates of equilibrated *Paramecium* applying a 0.6 V/cm voltage gradient. **A.** Down ($n=1512$) and Up rates ($n=1552$) cover a wide range of individual velocities. Note that a positive shift of the Down-rates with respect to the Up-rates applies to all velocities. **B.** Horizontal swimming rates. Proximal ($n=729$) corresponds to Down, and Distal ($n=859$) to Up. Comparison with (**A**) shows that swimming rate distributions are unrelated to gravity

in the presence and absence of the voltage gradient were identical, however, suggesting that cell immobilization was sufficiently complete for safe assessment of sedimentation. Immobilized cells were not moved in voltage gradients up to 2 V/cm. This excludes, together with the observations mentioned above, the existence of a significant amount of electrophoresis in immobilized and live paramecia during their exposure to the weak voltage gradient.

Rate of sedimentation. Cells sedimented in a wide range of velocities 0.035 to 0.345 mm/s (Fig. 13). The median of the distribution was 0.084 mm/s ($n=1362$, Table 2). Statistical analysis shows the median of sedimentation rate (of our 2-day cell populations in experimental solution) is stable down to $n=100$; even with $n=25$, the median varied between 0.067 and 0.097 mm/s only.

Isolation of the gravity-induced kinetic component. With the values of D (downward rate), U (upward rate) and S (sedimentation rate) determined, Eq. (14) yields an absolute value of Δ of 0.038 mm/s which eliminates model #1 in addition to the statistical test mentioned previously. The sign of Δ is negative excluding model #2 and confirming model #3. A negative value of 0.038 mm/s means that the mean gravikinetic component antagonizes sedimentation.

Model #3 assumes, by electrophysiological reasoning, that the value of Δ is the arithmetic mean of two independent subcomponents, Δ_a and Δ_p (equation 10). Application of equations (8) and (9), that is, inclusion of the value of P (unbiased horizontal propulsion) into calculations, isolates the scalar values of $\Delta_a = 0.070$ mm/s, and of $\Delta_p = 0.005$ mm/s (Table 2). These data suggest that downward swimming cells slow down by Δ_a so as to largely compensate the effect of sedimentation (0.084 mm/s), and upward swimming cells slightly speed up by Δ_p. The value of Δ_p is small and may be non-existent.

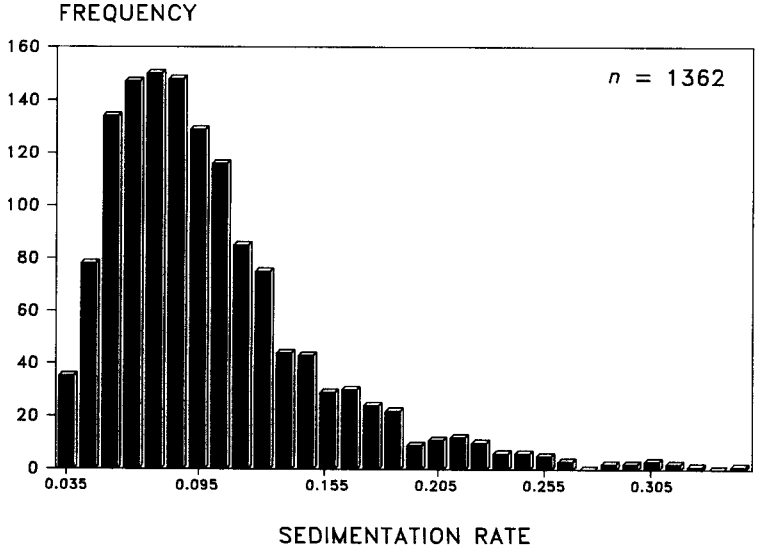

Fig. 13. Distribution of rates of sedimentation. The histogram shows a non-Gaussian distribution, the median of which is 0.084 mm/s (Table 2)

Discussion

The present paper is the first quantitative and statistically secured account of a physiological component in gravitaxis of *Paramecium*. The existence of a gravikinetic component was suggested by previous experiments (Mogami et al. 1988a; Baba et al. 1989), and was postulated on theoretical grounds (Machemer 1989). Mogami et al. (1988a) observed a minor reduction of the swimming rate of *Paramecium* during free fall ($n=9$), and this reduction was more pronounced in cells swimming upward ($n=6$). A tendency in *Paramecium* for active compensation of sedimentation was also inferred from the behaviour of slowly swimming cells at 1 G, and of fast swimming cells in the presence of hypergravity ($\geq 3\,G$; Baba et al. 1989). Anoxic conditions raised the swimming velocity and improved gravitaxis in *Paramecium* (Hemmersbach-Krause et al. 1990); it remains to be determined, if gravitaxis profited from the kinetic response or was specifically affected by anoxia. A strategy for isolation of a gravikinetic component according to Eq. (14) was proposed by Machemer (1989), and preliminary results confirming the existence of this component were presented by Machemer-Röhnisch (1989).

We attempt to further secure the results of the present paper by combination of the mass-cell approach with an effort to control a variety of circumstantial parameters such as culture conditions, temperature, symmetry of the chamber, ionic equilibration, gas exchange, mechanical disturbances, electrophoresis. Our experimental design, subtraction of upward and downward swimming rates, further eliminates potential biasing factors such as effects of the electric DC field on swimming, and bioconvection. We sometimes observed phenomena resembling convection in sedimenting aggregates of Ni-treated immobile cells. Trajectories of these records were discarded. Convection was not observed in isolated immobile or active paramecia. If bioconvection nevertheless did occur in cathodally swimming cells, this artefact is cancelled due to the subtraction procedure.

Our data analysis suggests that the motor responses of individual paramecia to gravity may vary. This is no surprise since in large populations of unsolicited cells, horizontal as well as vertical swimming rates cover a wide range (Fig. 12), and so do individual sedimentation rates (Fig. 13). According to experimental experience, depolarizing and hyperpolarizing mechanoreceptor currents scatter in individual specimens (Ogura and Machemer 1980; Machemer-Röhnisch and Machemer 1984); similar conditions may apply to gravireception. The presumed individual variability in electric membrane steady-state conditions (size of leakage conductance) and sensitivity (type and number of channels available for gravireception) can explain, why some cells swam actively downward (Fig. 10A) exceeding rates of upward swimmers by up to 40% (Fig. 10B). Individual variability of experimental cells cautions the experimenter to draw generalizing conclusions from too small populations of cells. Our present data are based on approximately 1000 different cells (some of our readings (n) may include the same cell over different intervals). Statistical analysis of these data shows that 400 cells would lead to reliable conclusions; for sedimentation 100 specimens would suffice.

We were not prepared to see the major effect of gravikinesis referred to depolarizing activation (of the presumed anterior gravireceptor) during downward swimming, whereas hyperpolarizing activation (of the presumed posterior gravireceptor) was minimal. The relevance of this difference may depend on the goodness of the value of unbiased active propulsion (P; Eqs. 8 and 9). We have assumed that P is reasonably approximated during horizontal swimming in the $1-G$ environment. The real value of P needs to be determined in the virtual absence of the gravity vector (such as during free fall or in orbit). If P was overestimated by only 3%, both Δ_a and Δ_p approximate Δ; the latter value remains unaffected by P (Eq. 14).

The sizes of Δ_a and Δ_p might have been altered by the voltage gradient which generated, for a 230 µm cell, a (maximal) 7 mV hyperpolarization at the posterior cell apex during upward swimming, and a (maximal) 7 mV depolarization at the anterior cell end during downward swimming. A voltage dependence of mechanoreceptor conductances (g_K, g_{Ca}) has been shown in *Stylonychia:* the K-dependent hyperpolarizing conductance (g_K) decreased at potentials more positive than the resting potential (V_{mr}), and the Ca-dependent depolarizing conductance (g_{Ca}) decreased with potentials negative to V_{mr} (see Machemer and Deitmer 1985). Extrapolation of these data to a hypothetical minor V-dependence of receptor conductances in *Paramecium* (about 1% change per mV shift in potential) would not apply to our voltage gradient of 0.6 V/cm; this size of gradient shifts the sensitive membrane to potentials which do not affect the conductance of the mechanoreceptor. A weak desensitizing effect of pre-hyperpolarization on the posterior mechanoreceptor (and, by inference, on Δ_p) cannot be excluded a priori because hyperpolarizing conditioning of the membrane slightly reduces the K driving force and the size of the hyperpolarizing receptor potential. V_{mr} approximates -30 mV, and E_K -90 mV for our experimental solution (Ogura and Machemer 1980).

Using the calculated sizes of Δ_a and Δ_p at face value, they make sense: starved cells which are little responsive to an upward reorienting mechanism (Taneda et al. 1987), or cells having unusual distributions of Ca and Mg phosphorous crystals (Kaneshiro and Rope 1989) and/or lipids (Cole et al. 1990), may obviate fast sedimentation by means of reduction of their downward swimming rate. Inversely, the significance of the kinetic response, Δ_a, decreases with a rising proportion of orientation in gravitaxis suggesting that these mechanisms can partly substitute each other.

Our results show that gravitaxis in *Paramecium* is a complex behaviour including orientational as well as kinetic responses. We employ coefficients for quantitative description of gravitaxis (Table 1) showing that this response is not all or none. Our taxis coefficient of -0.23 suggests, however, that a cell population has a slow net upward drift. The proportion of the orientational component in establishing gravitaxis, as compared to the

kinetic component, appears to be in the order of 9/10 versus 1/10. The kinetic component potentially rises to a proportion of about 1/4 of gravitaxis in downward swimming cells.

In establishing the existence of a physiologically mediated response to graviy, we are not claiming that gravitaxis is based on gravisensation only. We would rather assume that the continuing controversy on *either* physical or physiological foundations of gravitaxis will eventually lead ad absurdum because both views are correct: (1) postulating gravisensation by interaction of cytoplasm and membrane (statocyst hypothesis; Loeb 1897; Lyon 1905; Koehler 1922), and (2) explaining gravitaxis in *Paramecium* on mechanical principles (Verworn 1889; Roberts 1970; Winet and Jahn 1974; Fukui and Asai 1985).

Acknowledgements. This work was supported by the Bundesminister für Forschung und Technologie, Federal Republic of Germany, grant 01QV88570 (to HM), and the Special Fund for Promoting Science and Technology, STA, Japan (to KT). We thank S. Hünnebeck, K. Obst and U. Schilken for technical assistance and Dr. P.F.M. Teunis for critically reading the manuscript.

References

Baba SA, Ooya M, Mogami Y, Okuno M, Izumi-Kurotani A, Yamashita M (1989) Gravireception in *Paramecium* with a note on digital image analysis of videorecords of swimming *Paramecium*. Biol Sci Space 3:285

Batschelet E (1981) Circular statistics in biology. In: Sibson R, Cohen JE (eds) Mathematics in biology. Academic Press, London New York Toronto Sydney San Francisco

Bean B (1984) Microbial geotaxis. In: Colombetti G, Lenci F (eds) Membranes and sensory transduction. Plenum Publishing Corporation, pp 163–198

Bräucker R, Machemer-Röhnisch S (1990) Gravitaxis in *Paramecium*: In search of a physiological component. J Protozool 37:60A, 281

Cole TA, Fok AK, Ueno MS, Allen AD (1990) Use of Nile Red as a rapid measure of lipid content in ciliates. Eur J Protistol 25:361–368

Fukui K, Asai H (1985) Negative geotactic behavior of *Paramecium caudatum* is completely described by the mechanism of buoyancy-oriented upward swimming. Biophys J 47:479–483

Haupt W (1962) Geotaxis. In: Ruhland W (ed) Encyclopedia of plant physiology, vol XVII, Physiology of movements. Springer, Berlin Heidelberg New York, pp 390–395

Kaneshiro ES, Rope AF (1989) *Paramecium tetraurelia* forms two different types of crystals. VIII Int Congr Protozool Abst 75 (11E1515)

Koehler O (1922) Über die Geotaxis von *Paramecium*. Arch Protistenk 45:1–94

Kuznicki L (1968) Behavior of *Paramecium* in gravitiy fields. I. Sinking of immobilized specimens. Acta Protozool 6:109–117

Loeb J (1897) Zur Theorie der physiologischen Licht- und Schwerkraftwirkungen. Pflügers Arch 66:439–466

Lyon EP (1905) On the theory of geotropism in *Paramecium*. Am J Physiol 14:421–432

Machemer H (1988a) Electrophysiology. In: Görtz HD (ed) *Paramecium*. Springer, Berlin Heidelberg New York, pp 185–215

Machemer H (1988b) Motor control of cilia. In: Görtz HD (ed) *Paramecium*. Springer, Berlin Heidelberg New York, pp 216–235

Machemer H (1988c) Galvanotaxis: Grundlagen der elektromechanischen Kopplung und Orientierung bei *Paramecium*. In: Zupanc GHK (ed) Praktische Verhaltensbiologie. Paul Parey, Berlin, pp 60–82

Machemer H (1989) A quantitative approach towards isolation of a gravity-induced motor response in *Paramecium* I: Theory. Biol Sci Space 3:286

Machemer H (1990a) Gravitaxis in *Paramecium*: An old problem reconsidered. J Protozool 37:61A, 291

Machemer H (1990b) Cellular behaviour modulated by ions: electrophysiological implications. J Protozool 36:463–487

Machemer H, Deitmer JW (1985) Mechanoreception in ciliates. Progr Sensory Physiol 5:81–118

Machemer H, De Peyer J (1977) Swimming sensory cells: Electrical membrane parameters, receptor properties and motor control in ciliated Protozoa. Verh Dtsch Zool Ges 1977:86–110

Machemer H, Ogura A (1979) Ionic conductances of membranes in ciliated and deciliated *Paramecium*. J Physiol 296:49–60

Machemer H, Sugino K (1989) Electrophysiological control of ciliary beating: A basis of motile behaviour in ciliated Protozoa. Comp Biochem Physiol 94A:365–374

Machemer-Röhnisch S (1989) A quantitative approach towards isolation of a gravity-induced motor response in *Paramecium* II: Methods and data. Biol Sci Space 3:286

Machemer-Röhnisch S, Machemer H (1984) Receptor current following controlled stimulation of immobile tail cilia in *Paramecium caudatum*. J Comp Physiol A 154:263–271

Mogami Y, Kimura T, Okuno M, Yamashita M, Baba SA (1988a) Free fall experiments on swimming behavior of ciliates. In: Proc 16. Int Symp Space Technology Science, pp 2351–2354

Mogami Y, Oobayashi C, Yamaguchi T, Ogiso Y, Baba SA (1988b) Negative geotaxis in sea urchin larvae: A possible role of mechanoreception in the late stages of development. J Exp Biol 137:141–156

Naitoh Y, Eckert R (1969) Ionic mechanisms controlling behavioral responses in *Paramecium* to mechanical stimulation. Science 164:963–965

Ogura A, Machemer H (1980) Distribution of mechanoreceptor channels in the *Paramecium* surface membrane. J Comp Physiol 135:233–242

Oka T, Nakaoka Y, Oosawa F (1986) Changes in membrane potential during adaptation to external potassium ions in *Paramecium caudatum*. J Exp Biol 126:111–117

Roberts AM (1970) Geotaxis in motile micro-organisms. J Exp Biol 53:687–699

Sachs L (1984) Angewandte Statistik. Springer, Berlin Heidelberg New York

Taneda K (1987) Geotactic behavior in *Paramecium caudatum*. I. Geotaxis assay of individual specimen. Zool. Sci 4:781–788

Taneda K, Miyata S, Shiota A (1987) Geotactic behavior in *Paramecium caudatum*. II. Geotaxis assay in a population of the specimens. Zool Sci 4:789–795

Verworn M (1889) Psychophysiologische Protistenstudien. Fischer, Jena

Winet H, Jahn TL (1974) Geotaxis in Protozoa. I. A propulsion gravity model for *Tetrahymena* (Ciliata). J Theor Biol 46:449–465